Intermolecular Vibrational Modes Speed Up Singlet Fission in Perylenediimide Crystals

ARTICLE *in* JOURNAL OF PHYSICAL CHEMISTRY LETTERS · DECEMBER 2014

Impact Factor: 7.46 · DOI: 10.1021/jz5023575

2 AUTHORS, INCLUDING:

F.C. Grozema
Delft University of Technology
129 PUBLICATIONS **3,721** CITATIONS

THE JOURNAL OF PHYSICAL CHEMISTRY Letters

Letter

pubs.acs.org/JPCL

Intermolecular Vibrational Modes Speed Up Singlet Fission in Perylenediimide Crystals

Nicolas Renaud* and Ferdinand C. Grozema*

Optoelectronic Materials Section, Department of Chemical Engineering, Delft University of Technology, Julianalaan 136, 2629BL Delft, The Netherlands

Supporting Information

ABSTRACT: We report numerical simulations based on a non-Markovian density matrix propagation scheme of singlet fission (SF) in molecular crystals. Ab initio electronic structure calculations were used to parametrize the exciton and phonon Hamiltonian as well as the interactions between the exciton and the intramolecular and intermolecular vibrational modes. We demonstrate that the interactions of the exciton with intermolecular vibrational modes are highly sensitive to the stacking geometry of the crystal and can, in certain cases, significantly accelerate SF. This result may help in understanding the fast SF experimentally observed in a broad range of molecular crystals and offers a new direction for the engineering of efficient SF sensitizers.

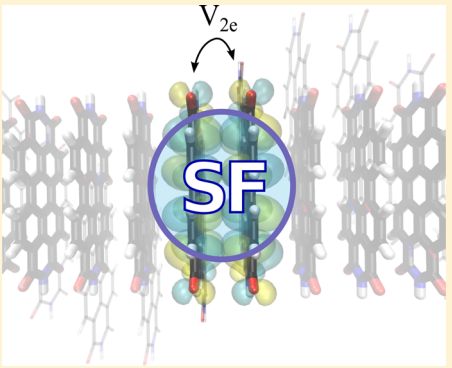

Designing cheap and efficient solar cells is an important challenge for the development of future technologies.[1] New strategies are therefore being sought to increase the maximum power conversion efficiency of solar cells beyond the Schockley−Queisser limit.[2] The utilization of singlet fission (SF) in molecular crystals is an interesting solution to reach that goal.[3] SF refers to a multielectron process by which a single absorbed photon leads to the formation of two triplet excitations localized on neighboring molecules.[4,5] Therefore, providing an efficient extraction of these excitations, SF sensitizers can potentially double the photocurrent obtained using traditional materials. Recently, a series of prototype devices exploiting SF have been created showing external quantum efficiencies exceeding 100%.[6−10] These outstanding results clearly demonstrate the potential of SF for future solar harvesting technologies.

Despite these impressive demonstrations and the observation of SF in a multitude of different molecular systems,[11−16] the intrinsic mechanism of SF is still poorly understood. Many theories, based on advanced electronic structure calculations[17−20] or density matrix propagation schemes on model dimer[21−25] or on a entire crystal,[26] have therefore been proposed to understand the microscopic events underlying SF. These calculations have permitted identification of two distinct pathways for the formation of the triplet states. One of these pathways is a two-step mechanism that involves charge-transfer (CT) states as intermediary species for the formation of triplet states.[5] Depending on the energetic configuration of the system, these CT states, where the two neighboring molecules are positively and negatively charged, can be used as either real or virtual intermediates during the SF dynamics. It has been theoretically demonstrated that this two-step mechanism can efficiently support SF, provided that the energies of the CT states are small enough and the different intermolecular electronic couplings are sufficiently large.[23,25] A one-step mechanism for SF that does not involve intermediary species has also been identified.[5,17,20,27] This direct mechanism is however mediated by a weak two-electron electronic coupling and is therefore often neglected. Recent studies have however demonstrated that the presence of this direct mechanism can significantly affect the rate of SF due to quantum interference between the two pathways[24,25] and may even fully support SF in selected cases.[27] Several studies have recently investigated the impact that crystal packing has on the efficiency of SF.[27,28] It has been shown that selected relative orientations between neighboring molecules lead to optimum intermolecular couplings and hence to a maximum SF efficiency. However, most of the studies have so far neglected the interaction between the exciton and the intermolecular vibrational modes. Berckelbach et. al have considered these vibrational modes in anthracene crystals and demonstrated that they play a minor role due to the large energy difference between the singlet and double triplet states.[29]

In this Letter, we study SF in molecular dimers using a non-Markovian density matrix propagation scheme.[30] The interactions of the exciton with the intramolecular and intermolecular vibrational modes, referred to as Holstein and Peierls interactions, respectively,[31] were explicitly included in the simulations. Holstein interactions have already been included in several recent articles using a Redfield approach.[23,25] As

Received: November 6, 2014
Accepted: December 24, 2014

DOI: 10.1021/jz5023575
J. Phys. Chem. Lett. 2015, 6, 360−365

expected, intramoelcular vibrational modes lead to an energy relaxation among the excitonic states that progressively drive the system to its thermal equilibrium. The interactions between the exciton and the intermolecular vibrational modes, that is, the Peierls interactions, have however received little attention. These vibrations induce fluctuations of the intermolecular couplings between neighboring molecules that might play an important role in the high charge carrier mobility observed for specific molecular crystals.[31,32] However, due to the low frequencies of the intermolecular vibrational modes, Peierls interactions are assumed to be very inefficient for energy relaxation and are therefore usually neglected in the study of SF.[29] We have evaluated the Peierls interactions for a series of similar molecular crystals using ab initio electronic structure calculations. We demonstrate here that subtle modification of the crystal packing geometry can have a significant impact of the interactions between the exciton and the intermolecular vibrational modes. It is then shown that while systems with large energy differences exhibit fission principally mediated by high-frequency intramolecular modes, the SF obtained in nearly isoenergetic systems can be facilitated by the interaction of the excitons with low-frequency intermolecular modes.

To account for the exciton−phonon (ex−ph) interactions during SF, the total Hamiltonian of the molecular dimer is decomposed as

$$\mathcal{H} = \mathcal{H}_{ex} + \mathcal{H}^{H}_{ph} + \mathcal{H}^{P}_{ph} + \mathcal{H}^{H}_{ex-ph} + \mathcal{H}^{P}_{ex-ph} \quad (1)$$

where $\mathcal{H}_{ex}$ is the excitonic Hamiltonian and $\mathcal{H}^{X}_{ph}$ is the phonon Hamiltonian of the intramolecular (X = H) and intermolecular (X = P) vibrational modes. Similarly, $\mathcal{H}^{X}_{ex-ph}$, with X = H,P represents the Holstein and Peierls interactions, respectively. Following previous studies,[4] we describe the molecular dimer by five excitonic states, two singlet excited states where only one of the two molecules is excited, two CT states, and the double triplet state where both molecules are in their triplet excited state. The excitonic Hamiltonian of the dimer then reads[4]

$$\mathscr{H}_{ex} = \begin{array}{c} \begin{matrix} |1\rangle & |2\rangle & |3\rangle & |4\rangle & |5\rangle \end{matrix} \\ \begin{pmatrix} E_{S_1S_0} & 0 & V_{LL} & -V_{HH} & V_{2e} \\ 0 & E_{S_0S_1} & -V_{HH} & V_{LL} & V_{2e} \\ V_{LL} & -V_{HH} & E_{CT} & 0 & \sqrt{\frac{3}{2}}V_{HL} \\ -V_{HH} & V_{LL} & 0 & E_{CT} & \sqrt{\frac{3}{2}}V_{LH} \\ V_{2e} & V_{2e} & \sqrt{\frac{3}{2}}V_{HL} & \sqrt{\frac{3}{2}}V_{LH} & E_{TT} \end{pmatrix} \end{array} \quad (2)$$

In this Hamiltonian, V_{HH} is the one-electron coupling between the HOMOs of the two molecules, V_{LL} is the coupling between the two LUMOs, and so on.[4] V_{2e} is the two-electron coupling supporting the direct SF pathway mentioned above.[4] As is usually done,[21,29] the excitonic coupling between S_1S_0 and S_0S_1 has been neglected, and the energy of the double triplet has been approximated by $E_{TT} = 2E_T$, where E_T is the triplet energy of an isolated molecule. These two approximations principally stem from the fact that the accuracy of the isolated singlet and triplet energies calculated at the TDDFT level of theory does not exceed the magnitude of these excitonic interactions, that is, a few tenths of an eV.[33,34] Note that the Hamiltonian in eq 2 can be expressed in a symmetry-adapted basis set by defining the states[28] $|S_\pm\rangle = (\sqrt{2})^{-1}(|1\rangle \pm |2\rangle)$ and $|CT_\pm\rangle = (\sqrt{2})^{-1}(|3\rangle \pm |4\rangle)$. In this basis, the state $|S_-\rangle$ is not directly coupled to the double triplet state, and only $|S_+\rangle$ presents a direct two-electron coupling with $|5\rangle$. Assuming an equal oscillator strength for the transitions between the ground state and S_1S_0 and S_0S_1, the state $|S_+\rangle$ should have the largest oscillator strength and therefore be close to the true excited state.

In its most general form, the ex−ph interaction Hamiltonian is given by $\mathcal{H}^{X}_{ex-ph} = \sum_m A^{X}_m \otimes [\sum_i \hbar\omega_i\lambda_i(b_i + b_i^\dagger)]^{X}_m$, with $b_i^\dagger$ (b_i) as the boson creation (annihilation) operator of the ith intramolecular (X = H) or intermolecular (X = P) mode, ω_i as the vibrational frequency of this mode, and λ_i as the corresponding ex−ph coupling. The operators A^{X}_m depend on the type of interactions considered. The Holstein interactions lead to site energy fluctuations and are therefore characterized by diagonal operators,[23] $A^{H}_m = |m\rangle\langle m|$. On the contrary, Peierls interactions induce fluctuations of the intermolecular couplings and are therefore characterized by nondiagonal operators. Both the one-electron couplings V_{XY} (X,Y = L,H) and the two-electron coupling V_{2e} are affected by the intermolecular vibrational modes. However, our calculations on perylenediimide (PDI) molecular crystals presented in the Supporting Information (SI), as well as others on pentacene crystals,[29] have shown that the fluctuations of the one-electron couplings are not strong enough to significantly impact the SF dynamics. We therefore focus here on the variations of V_{2e} induced by intermolecular vibrational modes and consequently set $A^{P}_1 = A^{P^\dagger}_2 = |1\rangle\langle 5|$ and $A^{P}_3 = A^{P^\dagger}_4 = |2\rangle\langle 5|$. Even though they are neglected in our calculations, we do not exclude that the fluctuations of the one-electron couplings may play an important role in the SF dynamics of specific molecular crystals. Finally, the free phonon Hamiltonian reads $\mathcal{H}^{X}_{ph} = [\sum_i \hbar\omega_i b_i^\dagger b_i]^{X}$.

Using these definitions, the master equation governing the dynamics of the excitonic density matrix can be written as[30]

$$\frac{d}{dt}\rho_{ex}(t) = -\frac{i}{\hbar}[\mathcal{H}_{ex}, \rho_{ex}(t)] + \sum_{X=H,P}\sum_{\omega,m}\gamma_X(\omega, t)\left(A^{X}_m(\omega)\rho_{ex}(t)A^{X}_m(\omega)^\dagger - \frac{1}{2}\{A^{X}_m(\omega)^\dagger A^{X}_m(\omega), \rho_{ex}(t)\}\right) \quad (3)$$

A detailed derivation of this equation as well as the exact definition of the operators $A^{X}_m(\omega)$ can be found in the SI. As it can bee seen from eq 3, the influences of the intermolecular (X = P) and intramolecular (X = H) vibrational modes on the excitonic dynamics are entirely described by the time-dependent relaxation rates $\gamma_X(\omega,t)$. As demonstrated in the SI, these rates are given by

$$\gamma_X(\omega, t) = 2\int_0^\infty d\nu\, \mathcal{J}_X(\nu)\left[[1 + n(\nu)]\frac{\sin(\omega - \nu)t}{\omega - \nu} + n(\nu)\frac{\sin(\omega + \nu)t}{\omega + \nu}\right] \quad (4)$$

where $n(\nu)$ is the Bose distribution and $\mathcal{J}_X(\nu)$ is the spectral density of the intra- (X = H) or inter- (X = P) molecular vibrational modes. Following previous work,[23,25] we assume that these spectral densities are accurately described by a Ohmic spectral density with a Lorentzian high-frequency cutoff[25,29]

$$\mathcal{J}_X(\omega) = 2\omega\frac{\lambda_X\Omega_X}{\omega^2 + \Omega_X^2} \quad (5)$$

DOI: 10.1021/jz5023575
J. Phys. Chem. Lett. 2015, 6, 360−365

The parameters for the Holstein and Peierls spectral densities are however very different from each other, with $\Omega_P \ll \Omega_H$ and $\lambda_P \ll \lambda_H$. Due to the off-resonant character of the Peierls interaction, the time-dependent relaxation rates $\gamma_P(\omega,t)$ can present large oscillations between positive and negative values leading to non-Markovian features in the SF dynamics. However, due to the weak values of the Peierls reorganization energy, these features are weak in the results presented below. Consequently, similar results should be obtained using a Markovian approach, such as the Redfield equation, where the relaxation rates are time-independent. The non-Markovian quantum jump (NMQJ) approach[30,35] was used to solve the dynamics generated by the master eq 3. A detailed presentation of the NMQJ and its application to a simple excitonic dimer can be found in the SI. It is shown in the SI that the NMQJ technique gives similar results as those obtained with the numerically exact hierarchical equations of motion technique.

We first investigate the impact of Peierls coupling during SF for arbitrary but realistic values of the Hamiltonian parameters. We hence fix $V_{LL} = -V_{HH} = 25$ meV, $V_{LH} = V_{HL} = 15$ meV, $V_{2e} = 1$ meV, $\lambda_H = 100\lambda_P = 50$ meV, and $\Omega_H = 10\Omega_P = 150$ meV. The energies E_{CT} and E_{TT} are then varied with respect of $E_{S_1S_0}$ to obtain an energy landscape favorable to a sequential (Seq) or to a superexchange (SpX) mechanism for SF. In the Seq regime, the energy of the CT states lies in between those of the singlet and double triplet states, $E_{TT} < E_{CT} < E_{S_1S_0}$. In that case, the CT states are significantly populated during the SF dynamics and are therefore a real intermediate species. On the contrary, in the SpX regime, the energy of the CT states is higher than those of the singlet and double triplet states, $E_{TT} < E_{S_1S_0} < E_{CT}$. In this case, the CT states are used as virtual intermediate states and are not populated during the SF dynamics. The initial state of the evolution was set to $|S_+\rangle$ and the temperature to 300 K. The population of the double triplet state obtained with these parameters after 1.0 ps of evolution is shown in Figure 1. The population obtained in the absence of Peierls coupling, that is, $\lambda_P = 0$, is also represented for comparison.

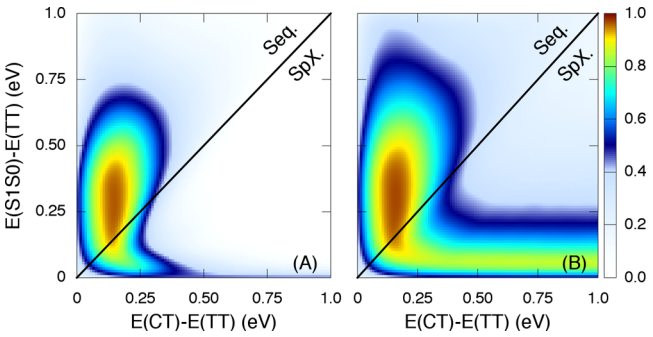

Figure 1. Double triplet state population obtained after 1 ps for λ_P = (A) 0 and (B) 0.5 meV. See the text for other parameters.

As seen in Figure 1A, in the absence of Peierls coupling, a subpicosecond SF can only be obtained in limited energetic conditions.[23] Hence, a fast SF can be obtained in the Seq regime (i.e., when the CT state energies lie in between those of the singlet and double triplet) and to a limited extent in the SpX regime, provided that $0 < E_{CT} - E_{S_1S_0} < 0.5$ eV. These results are in good agreement with those previously obtained via a Redfield approach.[29] As seen in Figure 1B, the presence of Peierls coupling significantly changes this picture. As a result of the ex−ph interactions with the intermolecular vibrational modes, a large population on the double triple state can be obtained in the SpX regime in less than 1 ps and for arbitrary large values of the CT states energy as long as $E_{S_1S_0} - E_{TT} \leq 0.25$ eV. The fastest SF is however obtained for $E_{S_1S_0} - E_{TT} \simeq \Omega_P$. For these values of the singlet and triplet energies, the emission of a single intermolecular phonon can directly relax the initial singlet excitation to a double triplet state without using the CT states. Consequently, a subpicosecond SF can be obtained using this new mechanism even if the CT state energies lie a few eV above those of the singlet state.

We now turn to the study of specific molecular crystals and investigate SF in PDI derivatives. It has been shown that tuning the stacking geometry of neighboring molecules in the crystals can optimize the charge carrier mobilities of PDI derivatives.[36,37] It is therefore interesting to understand how the relative orientation of neighboring molecules impacts the SF dynamics.[14,25,27] Experimental[38] and theoretical[39] works have indicated that PDIs present a very favorable energetic configuration for SF with $E_{S_1S_0} \simeq E_{TT}$. This is in strong contrast with most SF sensitizers for which the energy difference between the singlet and triplet can be relatively large.[40] Consequently, PDIs are potential candidates to observe a strong influence of the intermolecular vibrational modes on the SF rate. Additionally, the functionalization of the PDIs with different groups can be used to engineer their stacking geometries in the crystal.[41] Such crystal structure engineering allows tuning of the intermolecular couplings between neighboring molecules without significantly affecting their individual electronic structures.[36,37,42] In continuation of our previous work,[25] we study here the four PDI derivatives shown in Figure 2.

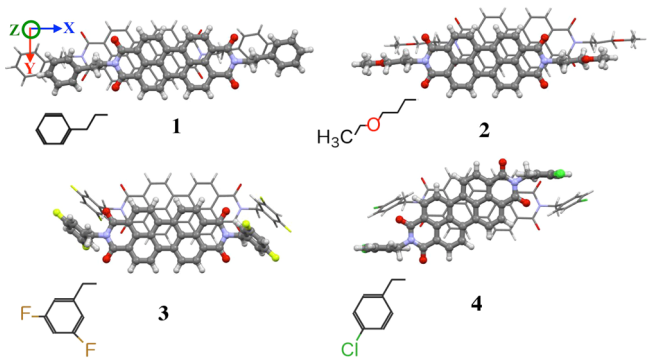

Figure 2. PDI derivatives studied in this Letter.

We have calculated the parameters of the excitonic and ex−ph Hamiltonians for these molecular dimers at the density functional level of theory. The results of these calculations are summarized in Table 1. The details of these calculations are given in the SI, and we only outline here the method adopted to compute the parameters related to the Peierls interactions, that is, Ω_P and λ_P.

To compute Ω_P and λ_P, we have considered an infinite one-dimensional chain of identical molecules and defined a unit cell containing two molecules. The ex−ph coupling strength with the intermolecular vibrational modes of the stack were then calculated in the rigid molecule approximation following[43]

DOI: 10.1021/jz5023575
J. Phys. Chem. Lett. 2015, 6, 360−365

Table 1. Values of the Exciton and Phonon Parameters for the Four PDI Derivatives Represented in Figure 2[a]

	$E_{S_1S_0}$[b]	E_{TT}[b]	E_{CT}[c]	V_{HH}[c]	V_{LL}[c]	V_{HL}[c]	V_{LH}[c]	V_{2e}[c]	Ω_H[b]	λ_H[b]	Ω_P	λ_P
1	2170	1900	3110	−125	145	−125	125	−0.42	150	77	20	0.09
2	2170	1900	2980	−108	−14	−35	35	−1.65	150	77	17	0.84
3	2170	1900	3390	−14	−100	0.8	−0.8	-1×10^{-3}	150	77	34	5×10^{-5}
4	2170	1900	3520	−35	22	1.2	−2.2	−1.1	150	77	27	0.14

[a]The energies are given in meV. [b]Values obtained for unsubstituted PDIs. [c]Values taken from ref [25].

$$L_P(\omega_m(k)) = \frac{1}{2M\omega_m^2(k)}\left(\frac{dV_{2e}}{dQ(\omega_m(k))}\right)^2_{Q=0} \quad (6)$$

In eq 6, $Q(\omega_m(k))$ is the vibrational coordinate of the mth vibrational mode with a wave vector k. M is the effective mass of the mode, set here at twice the mass of PDI, and $\omega_m(k)$ is its frequency. Three bands, corresponding to molecular displacements along the long axis (X), short axis (Y), or interplanar axis (Z) of the dimer were considered. The frequency of the modes were calculated in the harmonic approximation, that is, $\omega_m(k) = 2(K_m/M)^{1/2}\sin(k)$, where the parameter K_m was extracted from the variations of the dimer binding energy near its equilibrium configuration. During these calculations, the coupling between inter- and intramolecular vibrational modes was neglected.[31] As a consequence, the intermolecular modes obtained here have no intramolecular character.

The values of $L_P(\omega_m(k))$ obtained for the molecules **1**−**4** are shown in Figure 3. As seen in this figure, the maximum values

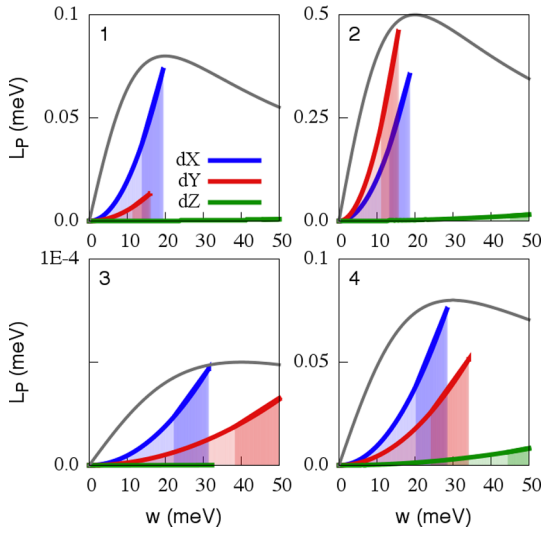

Figure 3. Peierls coupling for the four PDIs studied here. The light (heavy) shaded area corresponds to acoustic (optical) vibrational modes. The corresponding spectral density is represented in each case by a gray line.

of $L_P(\omega_m(k))$ vary significantly from one molecule to another, ranging from 0.5 meV for **2** to 0.5×10^{-4} meV for **3**. These large variations of $L_P(\omega_m(k))$ are principally due to strong differences obtained for dV_{2e}/dQ for the different compounds. Additionally, the values of $L_P(\omega_m(k))$ obtained for a given molecule vary strongly depending on the intermolecular vibrational modes considered. As seen in the SI, the variations of V_{2e} are not much larger along the Z directions than those in the X−Y plane. As the oscillation frequencies of the intermolecular vibrational modes are larger in the Z direction than those in the X−Y plane, the reorganization energies of the compression modes tend to be smaller than those of the shearing modes. The values of Ω_P and λ_P were then extracted from these calculations by fitting the spectral density given by eq 5 to these ex−ph couplings. The resulting values are reported in Table 1, and the corresponding spectral densities are shown in Figure 3. As seen in this figure, the value of λ_P obtained for **3** is much smaller than those obtained for the three other molecules studied here. As demonstrated in the SI, this small value of λ_P is due to the very weak variations of V_{2e} around the equilibrium geometry of **3**.

We then calculated the excitonic dynamics for compounds **1**−**4** using the parameters reported in Table 1 and the initial state $|S_+\rangle$. The corresponding SF dynamics obtained with the NMQJ approach are shown in Figure 4. In each case, the

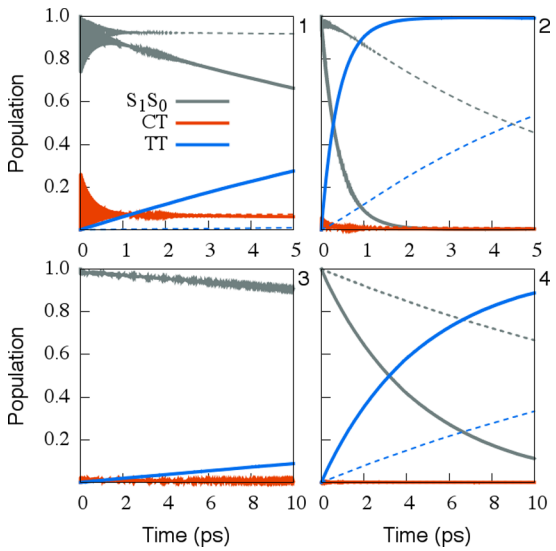

Figure 4. Population dynamics of PDIs **1**−**4** with (plain lines) and without (dashed lines) Peierls coupling. S_1S_0 represents the population of both singly excited states, CT the population of both CT states, and TT the population of the double triplet state.

dynamics obtained with and without Peierls ex−ph coupling are shown for comparison. In the case of **3**, the Peierls coupling is too weak for the intermolecular vibrational mode to affect the SF dynamics. As a result, the populations obtained with and without accounting for Peierls interactions are identical. On the contrary, the introduction of the Peierls couplings in the calculation significantly improves the SF dynamics obtained for **1**, **2**, and **4**. For example, in the case of **2**, the SF rate increases from 0.14 ps^{-1} for $\lambda_P = 0$ meV to 2.43 ps^{-1} for $\lambda_P = 0.84$ meV. This 20-fold increase of the SF rate is entirely due to the relatively large value of λ_P obtained for this compound. Similarly, in the case of **4**, a 5-fold increase of the SF rate was obtained going from 0.04 ps^{-1} in the absence of Peierls coupling to 0.21 ps^{-1} for $\lambda_P = 0.14$ meV.

DOI: 10.1021/jz5023575
J. Phys. Chem. Lett. 2015, 6, 360−365

As seen in Table 1, **1** presents large values of the one-electron intermolecular couplings and should therefore present a fast SF dynamics supported by the mediated pathway through the CT states. However, due the fact that $V_{LH} = -V_{HL}$, interference effects almost entirely suppress this mediated pathway, leaving only the direct pathway for the generation of the double triplet sate. As a consequence, the introduction of the Peierls couplings significantly affects the SF rate obtained for **1**. The SF rate hence goes from 0.002 ps^{-1} for $\lambda_P = 0$ meV to 0.067 ps^{-1} for $\lambda_P = 0.09$ meV, a 30-fold increase. Note that if V_{HL} would be equal to V_{LH} instead of being opposite to it, SF would occur in a few hundred femtoseconds and would not be affected by the intermolecular vibrational modes.[25]

We would like to stress here that the impact of the Peierls couplings on the SF dynamics depends on the choice of the initial state and on the spectral density assumed for the intermolecular vibrational modes. As shown in the SI, choosing an initial state different from $|S_+\rangle$ generally leads to less pronounced effects of the Peierls coupling. In particular, the Peierls couplings affect only marginally the SF dynamics of all compounds when the initial state is set to $|S_-\rangle$ as this state is not directly coupled with the double triplet state. The large effect of the Peierls couplings on the SF dynamics that is reported in Figure 4 represents therefore an upper limit to what one would obtain in the absence of control over the initial excitation. Similarly, the impact of the Peierls interaction can be reduced by the utilization of a bath spectral density that is different from the one given by eq 5, which presents a high-frequency tail. If the mixing between inter- and intramolecular vibrational modes can lead to high-frequency modes with a significant Peierls coupling,[31] most intermolecular modes present a low frequency. As demonstrated in the SI, the effect of the Peierls couplings only appears for $E_{S_1S_0} - E_{TT} < 100$ meV if a narrower density of states is assumed for the intermolecular vibrational modes.

In this Letter, we have demonstrated that the modulations of the two-electron coupling induced by the intermolecular vibrational modes of a molecular crystal can significantly affect the rate of SF. Several conditions must however be respected for these ex−ph couplings to be important. First, the energy difference between the singlet state and the double triplet state should not be too large compared to the central frequency of the intermolecular vibrational modes. The energy of the CT states should then be relatively high and the one-electron couplings relatively small to limit the influence of the indirect mechanism. Finally, the two-electron coupling should present large variations around the equilibrium position of the molecular dimer. As demonstrated in this Letter, selected PDI derivatives present all of these conditions simultaneously. The SF rates obtained for these molecular dimers are consequently sensitive to the presence of Peierls coupling. A significant increase of the SF rate, of about 1 order of magnitude, was then obtained for selected compounds. These results shed a new light on the role of the intermolecular vibrational modes during SF and may help to rationalize the subpicosecond SF rate experimentally measured for selected molecular crystals despite the large values of their CT state energies.

■ ASSOCIATED CONTENT

Supporting Information

Derivation of eq 3, the master equation; application of the NMQJ approach to an excitonic dimer; symmetry-adapted basis set; electronic structure calculations for the PDI dimers; fluctuation of the one-electron coupling; impact of the initial state; and impact of the spectral density. This material is available free of charge via the Internet at http://pubs.acs.org.

■ AUTHOR INFORMATION

Corresponding Authors

*E-mail: n.renaud@tudelft.nl (N.R.).
*E-mail: f.c.grozema.tudelft.nl (F.C.G.).

Notes

The authors declare no competing financial interest.

■ ACKNOWLEDGMENTS

The research leading to these results has received funding from the European Research Council under the European Union's Seventh Framework Programme (FP7/2007-2013)/ERC Grant Agreement Number 240299.

■ REFERENCES

(1) Nozik, A. J. Nanoscience and Nanostructures for Photovoltaics and Solar Fuels. *Nano Lett.* **2010**, *10*, 2735−2741 PMID: 20597472..
(2) Schockley, W.; Queisser, H. J. Detailed Balance Limit of Efficiency of p−n Junction Solar Cells. *J. Appl. Phys.* **1961**, *32*, 510.
(3) Hanna, M. C.; Nozik, A. Solar Conversion Efficiency of Photovoltaic and Photoelectrolysis Cells with Carrier Multiplication Absorbers. *J. Appl. Phys.* **2006**, *100*, 074510.
(4) Smith, M. B.; Michl, J. Singlet Fission. *Chem. Rev.* **2010**, *110*, 6891.
(5) Smith, M. B.; Michl, J. Recent Advances in Singlet Fission. *Annu. Rev. Phys. Chem.* **2013**, *64*, 361−86.
(6) Jadhav, P. J.; Brown, P. R.; Thompson, N.; Wunsch, B.; Mohanty, A.; Yost, S. R.; Hontz, E.; Van Voorhis, T.; Bawendi, M. G.; Bulovic, V.; Baldo, M. A. Triplet Exciton Dissociation in Singlet Exciton Fission Photovoltaics. *Adv. Mater.* **2012**, *24*, 6169−74.
(7) Reusswig, P. D.; Congreve, D. N.; Thompson, N. J.; Baldo, M. A. Enhanced External Quantum Efficiency in an Organic Photovoltaic Cell via Singlet Fission Exciton Sensitizer. *Appl. Phys. Lett.* **2012**, *101*, 113304.
(8) Ehrler, B.; Walker, B. J.; Bohm, M. L.; Wilson, M. W.; Vaynzof, Y.; Friend, R. H.; Greenham, N. C. In Situ Measurement of Exciton Energy in Hybrid Singlet-Fission Solar Cells. *Nat. Commun.* **2012**, *3*, 1019.
(9) Jadhav, P. J.; Mohanty, A.; Sussman, J.; Lee, J.; Baldo, M. A. Singlet Exciton Fission in Nanostructured Organic Solar Cells. *Nano Lett.* **2011**, *11*, 1495−1498.
(10) Congreve, D. N.; Lee, J.; Thompson, N. J.; Hontz, E.; Yost, S. R.; Reusswig, P. D.; Bahlke, M. E.; Reineke, S.; Van Voorhis, T.; Baldo, M. A. External Quantum Efficiency above 100% in a Singlet-Exciton-Fission-Based Organic Photovoltaic Cell. *Science* **2013**, *340*, 334−337.
(11) Rao, A.; Wilson, M. W. B.; Hodgkiss, J. M.; Albert-Seifried, S.; Bassler, H.; Friend, R. H. Exciton Fission and Charge Generation via Triplet Excitons in Pentacene/C_{60} Bilayers. *J. Am. Chem. Soc.* **2010**, *132*, 12698−12703.
(12) Muller, A. M.; Avlasevich, Y. S.; Shoeller, W. W.; Mullen, K.; Bardeen, C. J. Exciton Fission and Fusion in Bis(tetracene) Moelcules with Different Covalent Linker Structure. *J. Am. Chem. Soc.* **2007**, *129*, 14240.
(13) Roberts, S. T.; McAnally, R. E.; Mastron, J. N.; Webber, D. H.; Whited, M. T.; Brutchey, R. L.; Thompson, M. E.; Bradforth, S. E. Efficient Singlet Fission Discovered in a Disordered Acene Film. *J. Am. Chem. Soc.* **2012**, *134*, 6388−6400.

DOI: 10.1021/jz5023575
J. Phys. Chem. Lett. 2015, 6, 360−365

(14) Eaton, S. W.; Shoer, L. E.; Karlen, S. D.; Dyar, S. M.; Margulies, E. A.; Veldkamp, B. S.; Ramanan, C.; Hartzler, D. A.; Savikhin, S.; Marks, T. J.; Wasielewski, M. R. Singlet Exciton Fission in Polycrystalline Thin Films of a Slip-Stacked Perylenediimide. *J. Am. Chem. Soc.* **2013**, *135*, 14701−14712.
(15) Chan, W.-L.; Ligges, M.; Jailaubekov, A.; Kaake, L.; Miaja-Avila, L.; Zhu, X.-Y. Observing the Multiexciton State in Singlet Fission and Ensuing Ultrafast Multielectron Transfer. *Science* **2011**, *334*, 1541−1545.
(16) Ma, L.; Zhang, K.; Kloc, C.; Sun, H.; Michel-Beyerle, M. E.; Gurzadyan, G. G. Singlet Fission in Rubrene Single Crystal: Direct Observation by Femtosecond Pump−Probe Spectroscopy. *Phys. Chem. Chem. Phys.* **2012**, *14*, 8307−8312.
(17) Zimmerman, P. M.; Bell, F.; Casanova, D.; Head-Gordon, M. Mechanism for Singlet Fission in Pentacene and Tetracene: From Single Exciton to Two Triplets. *J. Am. Chem. Soc.* **2011**, *133*, 19944−19952.
(18) Zimmerman, P. M.; Zhang, Z.; Musgrave, C. B. Singlet Fission in Pentacene through Multiexciton Quantum States. *Nat. Chem.* **2010**, *2*, 648−652.
(19) Parker, S. M.; Seideman, T.; Ratner, M. A.; Shiozaki, T. Model Hamiltonian Analysis of Singlet Fission from First Principles. *J. Phys. Chem. C* **2014**, *118*, 12700−12705.
(20) Havenith, R. W.; Gier, H.; Broer, R. Explorative Computational Study of the Singlet Fission Process. *Mol. Phys.* **2012**, *1*, 1−10.
(21) Greyson, E. C.; Vura-Weiss, J.; Michl, J.; Ratner, M. A. Maximising Singlet Fission in Organic dimers: Theoretical Investigation of Triplet Yield in the Regime of Localized Excitation and Fast Coherent Electron Transfer. *J. Phys. Chem. B* **2010**, *114*, 14168.
(22) Teichen, P. E.; Eaves, J. D. A Microscopic Model of Singlet Fission. *J. Phys. Chem. B* **2012**, *116*, 11473−11481.
(23) Berkelbach, T. C.; Hybertsen, M. S.; Reichman, D. R. Microscopic Theory of Singlet Exciton Fission. I. General Formulation. *J. Chem. Phys.* **2013**, *138*, 114102.
(24) Tao, G. Electronically Nonadiabatic Dynamics in Singlet Fission: A Quasi-Classical Trajectory Simulation. *J. Phys. Chem. C* **2014**, *118*, 17299−17305.
(25) Mirjani, F.; Renaud, N.; Gorczak, N.; Grozema, F. C. Theoretical Investigation of Singlet Fission in Molecular Dimers: The Role of Charge Transfer States and Quantum Interference. *J. Phys. Chem. C* **2014**, *118*, 14192−14199.
(26) Berkelbach, T. C.; Hybertsen, M. S.; Reichman, D. R. Microscopic Theory of Singlet Exciton Fission. III. Crystalline Pentacene. *J. Chem. Phys.* **2014**, *141*, 074705.
(27) Renaud, N.; Sherratt, P. A.; Ratner, M. A. Mapping the Relation between Stacking Geometries and Singlet Fission Yield in a Class of Organic Crystals. *J. Phys. Chem. Lett.* **2013**, *4*, 1065−1069.
(28) Wang, L.; Olivier, Y.; Prezhdo, O. V.; Beljonne, D. Maximizing Singlet Fission by Intermolecular Packing. *J. Phys. Chem. Lett.* **2014**, *5*, 3345−3353.
(29) Berkelbach, T. C.; Hybertsen, M. S.; Reichman, D. R. Microscopic Theory of Singlet Exciton Fission. II. Application to Pentacene Dimers and the Role of Superexchange. *J. Chem. Phys.* **2013**, *138*, 114103.
(30) Piilo, J.; Maniscalco, S.; Härkönen, K.; Suominen, K.-A. Non-Markovian Quantum Jumps. *Phys. Rev. Lett.* **2008**, *100*, 180402.
(31) Girlando, A.; Grisanti, L.; Masino, M.; Bilotti, I.; Brillante, A.; Della Valle, R. G.; Venuti, E. Peierls and Holstein Carrier-Phonon Coupling in Crystalline Rubrene. *Phys. Rev. B* **2010**, *82*, 035208.
(32) Troisi, A.; Orlandi, G. Charge-Transport Regime of Crystalline Organic Semiconductors: Diffusion Limited by Thermal Off-Diagonal Electronic Disorder. *Phys. Rev. Lett.* **2006**, *96*, 086601.
(33) Spano, F. C. Excitons In Conjugated Oligomer Aggregates, Films, and Crystals. *Annu. Rev. Phys. Chem.* **2006**, *57*, 217−243.
(34) Yamagata, H.; Norton, J.; Hontz, E.; Olivier, Y.; Beljonne, D.; Brédas, J. L.; Silbey, R. J.; Spano, F. C. The Nature of Singlet Excitons in Oligoacene Molecular Crystals. *J. Chem. Phys.* **2011**, *134*, -.
(35) Rebentrost, P.; Chakraborty, R.; Aspuru-Guzik, A. Non-Markovian Quantum Jumps in Excitonic Energy Transfer. *J. Chem. Phys.* **2009**, *131*, 184102.
(36) Vura-Weiss, J.; Ratner, M. A.; Wasielewski, M. R. Geometry and Electronic Coupling in Perylenediimide Stacks: Mapping Structure−Charge Transport Relationships. *J. Am. Chem. Soc.* **2010**, *132*, 1738.
(37) Delgado, M. C. R.; Kim, E.-G.; da Silva Filho, D. A.; Bredas, J.-L. Tuning the Charge-Transport Parameters of Perylene Diimide Single Crystals via End and/or Core Functionalization: A Density Functional Theory Investigation. *J. Am. Chem. Soc.* **2010**, *133*, 3375−3387.
(38) Ford, W. E.; Kamat, P. V. Photochemistry of 3,4,9,10-Perylenetetracarboxylic Dianhydride Dyes. 3. Singlet and Triplet Excited-State Properties of the Bis(2,5-di-tert-butylphenyl)imide Derivative. *J. Phys. Chem.* **1987**, *91*, 6373−6380.
(39) Quartarolo, A. D.; Chiodo, S. G.; Russo, N. A TDDFT Investigation of Bay Substituted Perylenediimides: Absorption and Intersystem Crossing. *J. Comput. Chem.* **2012**, *33*, 1091−1100.
(40) Paci, I.; Johson, J. C.; Cheng, X.; Rana, G.; Popovic, D.; David, D. E.; Nozik, A. J.; Ratner, M. A.; Michl, J. Singlet Fission for Dye-Sensitized Solar Cells: Can a Suitable Sinsitizer Be Found ? *J. Am. Chem. Soc.* **2006**, *128*, 16546.
(41) Balkrishanan, K.; Datar, A.; Naddo, T.; Huang, J.; Oitker, R.; Yen, M.; Zhao, J.; Zang, L. Effect of Side-Chain Substituents on Self-Assembly of Perylene Diimide Molecules: Morphology Control. *J. Am. Chem. Soc.* **2006**, *128*, 7391.
(42) Gunbas, D. D.; Xue, C.; Patwardhan, S.; Fravventura, M. C.; Zhang, H.; Jager, W. F.; Sudholter, E. J. R.; Siebbeles, L. D. A.; Savenije, T. J.; Jin, S.; Grozema, F. C. High Charge Carrier Mobility and Efficient Charge Separation in Highly Soluble Perylenetetracarboxyl-Diimides. *Chem. Commun.* **2014**, *50*, 4955−4958.
(43) Coropceanu, V.; Cornil, J.; da Silva Filho, D. A.; Olivier, Y.; Silbey, R.; Brédas, J.-L. Charge Transport in Organic Semiconductors. *Chem. Rev.* **2007**, *107*, 926−952 PMID: 17378615..

DOI: 10.1021/jz5023575
J. Phys. Chem. Lett. 2015, 6, 360−365